

# Superconductivity in self-flux-synthesized single crystalline $R_2Pt_3Ge_5$ ( $R = La, Ce, Pr$ )\*

Q Sheng(盛琪)<sup>1</sup>, J Zhang(张建)<sup>1</sup>, K Huang(黄百畅)<sup>1,†</sup>, Z Ding(丁兆峰)<sup>1</sup>,  
X Peng(彭小冉)<sup>1</sup>, C Tan(谭程)<sup>1</sup>, and L Shu(苴蕾)<sup>1,2,‡</sup>

<sup>1</sup>State Key Laboratory of Surface Physics, Department of Physics, Fudan University, Shanghai 200433, China

<sup>2</sup>Collaborative Innovation Center of Advanced Microstructures, Nanjing 210093, China

(Received 28 November 2016; revised manuscript received 16 February 2017; published online 30 March 2017)

In order to study the basic superconductivity properties of  $Pr_2Pt_3Ge_5$ , we synthesized the single crystalline samples by the Pt–Ge self-flux method.  $R_2Pt_3Ge_5$  ( $R = La, Ce$ ) were also grown for a systematic study. Zero-resistivity was observed in both the La- and Pr-based samples below the reported superconducting transition temperatures. However, magnetic susceptibility measurements showed low superconductivity volume fractions in both  $La_2Pt_3Ge_5$  and  $Pr_2Pt_3Ge_5$  (less than 2%).  $Ce_2Pt_3Ge_5$  did not show any signature of superconductivity. From the specific heat measurements, we did not observe a superconducting transition peak in  $Pr_2Pt_3Ge_5$ , suggesting that it is not a bulk superconductor. The magnetic susceptibility and heat capacity measurements revealed two antiferromagnetic (AFM) orders in  $Pr_2Pt_3Ge_5$  at  $T_{N1} = 4.2$  K and  $T_{N2} = 3.5$  K, as well as a single AFM transition at  $T_N = 3.8$  K in  $Ce_2Pt_3Ge_5$ .

**Keywords:** superconductivity, antiferromagnetism, heavy fermion behavior

**PACS:** 74.25.Ha, 75.50.Ee

**DOI:** 10.1088/1674-1056/26/5/057401

## 1. Introduction

The  $R_2T_3X_5$  family ( $R$ ,  $T$ , and  $X$  stand for rare-earth elements, transition metals, and s–p metals, respectively) provides a vast platform for studying superconductivity, heavy fermion (HF) behavior, Kondo effect, magnetic orders, and many other novel phenomena.<sup>[1–3]</sup> The interplay between magnetic phase transitions and superconductivity in this family catches the interest of researchers. Compared to the superconductivity transition temperatures  $T_c$  reported in the cuprate superconductors or the iron-based superconductors,<sup>[4,5]</sup>  $T_c$  in this family is relatively low, with the highest  $T_c$  of 6.3 K reported in the multiband superconductor  $Lu_2Fe_3Si_5$ .<sup>[6,7]</sup> Remarkably, pressure induced heavy fermion superconductivity was found in the antiferromagnet  $Ce_2Ni_3Ge_5$ ,<sup>[8]</sup> raising more doubt about the relation between superconductivity and magnetism in this system. The discovery of superconductivity in antiferromagnetic (AFM)  $R_2T_3X_5$  compounds will definitely fulfill the magnetic-superconductivity phase diagram of this 2–3–5 family as well as the heavy fermion superconductors.<sup>[9]</sup> Recently,  $Pr_2Pt_3Ge_5$  was reported to have  $T_c \sim 8$  K,<sup>[6]</sup> which is the highest in the 2–3–5 family. At even lower temperatures, neutron scattering measurements found two AFM transitions, which are completely decoupled from the superconductivity in this compound.<sup>[10]</sup> In addition, Kondo screening of the magnetic Pr ions was also found, indicating the possibility of heavy fermion superconductivity (HFSC) for this compound, however the electric specific heat coefficient  $\gamma_n$  was not reported.<sup>[6]</sup>

Pr-based HFSCs are very rare, as the majority of heavy

fermion systems are U- or Ce-based compounds.<sup>[11,12]</sup> Therefore, the observation of superconductivity in  $Pr_2Pt_3Ge_5$  is particularly interesting as a potential new Pr-based HF superconductor. It is speculated that HFSC is unlikely to occur in the Pr-based compounds, as the singlet ground state does not support the degeneracy to form an HF ground state.<sup>[11]</sup> The discovery of HFSC in  $PrOs_4Sb_{12}$ , with electronic specific heat coefficient  $\gamma_n \sim 0.5$  J·mol<sup>−1</sup>·K<sup>−2</sup>, is thus very intriguing.<sup>[13]</sup> It was proposed that  $PrOs_4Sb_{12}$  has a huge hybridization among its first excited triplet  $\Gamma_4^{(2)}$  crystal-electric field (CEF) split state, the  $\Gamma_1$  and conduction electrons, leading to the emergence of the HF behavior.<sup>[11,14]</sup>

The reported  $T_c$  of  $Pr_2Pt_3Ge_5$  is  $\sim 8$  K, which is very close to that of the recently discovered Pt–Ge skutterudite  $PrPt_4Ge_{12}$ .<sup>[15–19]</sup> Also, a low superconductivity volume fraction was obtained from the meissner effect measurements.<sup>[6]</sup> These features raise the possibility that superconductivity occurs from the impurity filled-skutterudite phase and the doubt about whether the reported superconductivity in  $Pr_2Pt_3Ge_5$  is intrinsic or not.

Therefore, we systematically characterize the basic properties of  $R_2Pt_3Ge_5$  ( $R = La, Ce, Pr$ ) of the 2–3–5 family by resistivity, magnetic susceptibility, and heat capacity measurements to determine (i) whether  $Pr_2Pt_3Ge_5$  is a heavy fermion compound, and (ii) the source of the superconductivity. Zero-resistance is found in  $R_2Pt_3Ge_5$  ( $R = La, Pr$ ) below the reported  $T_c$  of  $\sim 8$  K.<sup>[6]</sup>  $Pr_2Pt_3Ge_5$  displays quite a low superconductivity volume fraction (less than 2 %) from the mag-

\*Project supported by the National Natural Science Foundation of China (Grant No. 11204041) and STCSM of China (Grant No. 15XD1500200).

†Present address: National High Magnetic Field Laboratory, Tallahassee, Florida 32310

‡Corresponding author. E-mail: leishu@fudan.edu.cn

netic susceptibility measurements. From the specific heat measurements, we find no jump near  $T_c$ . Therefore, our results suggest that the superconductivity in  $\text{Pr}_2\text{Pt}_3\text{Ge}_5$  is not bulk. Moreover, the relatively small values of  $\gamma_n$  provide evidence that  $R_2\text{Pt}_3\text{Ge}_5$  ( $R = \text{La}, \text{Ce}, \text{Pr}$ ) are not heavy fermion compounds.

## 2. Experimental details

Single crystalline samples of  $R_2\text{Pt}_3\text{Ge}_5$  ( $R = \text{La}, \text{Ce}, \text{Pr}$ ) were synthesized using the Pt–Ge self-flux method as described in Ref. [6]. The starting materials La/Ce (99.9%), Pr (99.5%) rods (Alfa Aesar), Pt shots (99.9%), and Ge pieces (Alfa Aesar 99.9999+%) were mixed with the stoichiometric ratio of 1:4:20. They were put in alumina crucibles before being sealed in a quartz tube. They were heated to 1130 °C and dwell at this temperature for 40 h before cooling down to 850 °C with a rate of 3 °C/h. X-ray diffraction (XRD) measurements were performed by using an x-ray diffractometer (D8 Advance, Bruker) with  $\text{Cu-K}\alpha$  radiation. Rietveld refinements were conducted on powder XRD patterns using the softwares GSAS<sup>[20]</sup> and EXPGUI.<sup>[21]</sup> The dc magnetization was measured by a Quantum Design superconducting quantum interference device. Four wire electrical resistivity measurements (2 K to 300 K) and specific heat measurements (2 K to 50 K) were performed in a Quantum Design physical properties measurement system Evercool II, with the specific heat measurements employing a standard thermal relaxation technique.

## 3. Results and discussion

For all of the  $R_2\text{Pt}_3\text{Ge}_5$  samples, the x-ray measurements reveal that they form in the  $\text{U}_2\text{Co}_3\text{Si}_5$ -type orthorhombic structure with space group  $Ibam$ , which can be viewed as a combination of the  $\text{CaBe}_2\text{Ge}_2$  and the  $\text{BaNiSi}_3$  structures.<sup>[22]</sup> The x-ray data are displayed in Fig. 1. The lattice parameters are summarized in Table 1, with values close to the results in Refs. [6] and [23]. The lattice parameters of  $\text{La}_2\text{Pt}_3\text{Ge}_5$ ,  $\text{Ce}_2\text{Pt}_3\text{Ge}_5$ , and  $\text{Pr}_2\text{Pt}_3\text{Ge}_5$  decrease as the atomic radius of the constituent rare-earth elements decreases. The single crystal XRD pattern of  $\text{Pr}_2\text{Pt}_3\text{Ge}_5$  with the incident beam oriented along the  $b$ -axis is displayed in Fig. 1(d).

Figure 2 shows the temperature dependence of resistivity  $\rho(T)$  measured in zero magnetic field for  $\text{Pr}_2\text{Pt}_3\text{Ge}_5$  and  $\text{Ce}_2\text{Pt}_3\text{Ge}_5$  single crystals along the  $c$ -axis. For the electrical resistivity measurements, we define  $T_c$  as the temperature at which the resistance drops to zero and find  $T_c = 7.8$  K for  $\text{Pr}_2\text{Pt}_3\text{Ge}_5$ , which is consistent with the previous work<sup>[6]</sup> and is almost the same as the  $T_c$  of  $\text{PrPt}_4\text{Ge}_{12}$ .<sup>[15]</sup>  $\rho(T)$  gives a residual resistivity ratio  $\rho(300 \text{ K})/\rho(8 \text{ K}) \simeq 3.9$ , slightly larger than that in the previous work.<sup>[6]</sup> Zero resistance is also found in  $\text{La}_2\text{Pt}_3\text{Ge}_5$  at 8.2 K (not shown here) while

$\text{Ce}_2\text{Pt}_3\text{Ge}_5$  does not transit into the superconducting state. The resistivity data are displayed in Fig. 2(b), where  $\text{Ce}_2\text{Pt}_3\text{Ge}_5$  shows a local minimum around  $\sim 15$  K followed by the upturn to the local maximum resistivity at  $\sim 7$  K. A sharp drop occurs at  $T_N = 3.5$  K, consistent with the Néel temperature determined from the magnetization measurements (will be discussed later). Such behaviors are similar to those observed in another Ce-based 2–3–5 compound,  $\text{Ce}_2\text{Ir}_3\text{Sn}_5$ .<sup>[24]</sup>

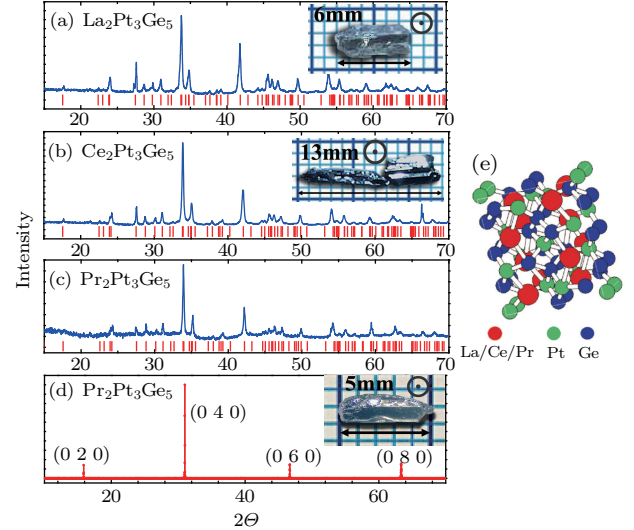


**Fig. 1.** (a)–(c) Powder XRD patterns of pulverized single crystals  $\text{La}_2\text{Pt}_3\text{Ge}_5$ ,  $\text{Ce}_2\text{Pt}_3\text{Ge}_5$ , and  $\text{Pr}_2\text{Pt}_3\text{Ge}_5$ , respectively. Tick marks below each pattern indicate the expected Bragg peaks for the refined  $\text{U}_2\text{Co}_3\text{Si}_5$ -type orthorhombic crystal structure. (d) The single crystal XRD pattern of  $\text{Pr}_2\text{Pt}_3\text{Ge}_5$  along the  $b$ -axis. The dotted circles shown in panels (a), (b), and (d) represent the direction of the  $b$ -axis. (e) The crystal structure of  $R_2\text{Pt}_3\text{Ge}_5$  ( $R = \text{La}, \text{Ce}, \text{Pr}$ ).

**Table 1.** Lattice parameters and unit cell volumes of  $R_2\text{Pt}_3\text{Ge}_5$  ( $R = \text{La}, \text{Ce}, \text{Pr}$ ).

	$a/\text{Å}$	$b/\text{Å}$	$c/\text{Å}$	$V/\text{Å}^3$
$\text{La}_2\text{Pt}_3\text{Ge}_5$	10.121(3)	11.998(1)	6.228(4)	756.28(1)
$\text{Ce}_2\text{Pt}_3\text{Ge}_5$	10.102(3)	11.888(4)	6.203(2)	744.93(1)
$\text{Pr}_2\text{Pt}_3\text{Ge}_5$	10.098(3)	11.852(2)	6.192(4)	741.07(1)

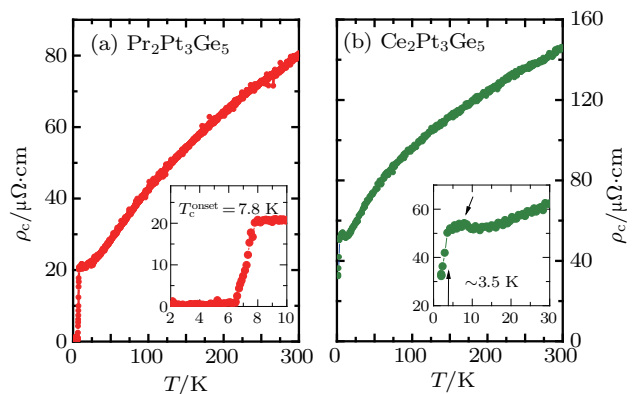
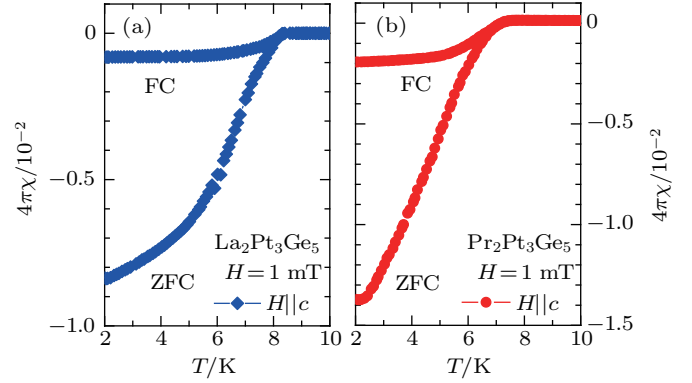


**Fig. 2.** (a) and (b) Temperature dependence of resistivity for  $\text{Pr}_2\text{Pt}_3\text{Ge}_5$  and  $\text{Ce}_2\text{Pt}_3\text{Ge}_5$  measured along the  $c$ -axis without an applied magnetic field, respectively. The inset in panel (a) highlights the low temperature resistivity, where the transition into the superconducting state is observed at  $T_c = 7.8$  K for  $\text{Pr}_2\text{Pt}_3\text{Ge}_5$ . The inset of panel (b) shows the low temperature resistivity of  $\text{Ce}_2\text{Pt}_3\text{Ge}_5$ , where an abrupt drop is observed at  $\sim 3.5$  K, which is consistent with the formation of the antiferromagnetic phase.

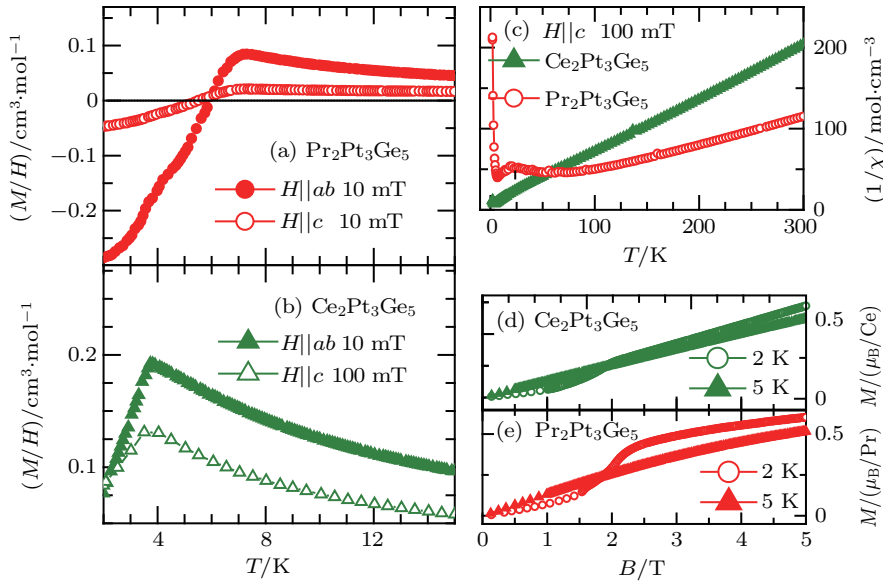
Full diamagnetization is one of the signature properties of bulk superconductivity. Therefore magnetization measurements at low fields were performed to determine the superconducting volume fraction. Figure 3 shows the zero-field-cooled (ZFC) and field-cooled (FC) dc-susceptibility of  $\text{La}_2\text{Pt}_3\text{Ge}_5$  and  $\text{Pr}_2\text{Pt}_3\text{Ge}_5$  with the magnetic field of  $H = 1$  mT applied along the  $c$ -axis. Both  $\text{La}_2\text{Pt}_3\text{Ge}_5$  and  $\text{Pr}_2\text{Pt}_3\text{Ge}_5$  show clear diamagnetic signals at  $T_c = 8.2$  K and 7.6 K, respectively, consistent with the results in Ref. [6]. However, when converted to the superconducting volume fractions, we find that they are less than 2% for both  $\text{La}_2\text{Pt}_3\text{Ge}_5$  and  $\text{Pr}_2\text{Pt}_3\text{Ge}_5$ , indicating the absence of bulk superconductivity.

Figure 4 shows the magnetization measurement results for  $\text{Pr}_2\text{Pt}_3\text{Ge}_5$  and  $\text{Ce}_2\text{Pt}_3\text{Ge}_5$ . Figure 4(a) is the magnetic susceptibility measured in applied magnetic fields of  $H = 10$  mT along the  $ab$ -plane and  $c$ -axis for  $\text{Pr}_2\text{Pt}_3\text{Ge}_5$ . The magnetization with the magnetic field applied along the  $c$ -axis is weaker than that parallel to the  $ab$ -plane, in agreement with

the anisotropy observed from neutron scattering.<sup>[10]</sup> For the  $H \parallel ab$  plane, two distinct downward kinks are observed at  $T_{N1} = 4.2$  K and  $T_{N2} = 3.5$  K, consistent with the results reported in Ref. [6].



**Fig. 3.** Meissner effect in (a)  $\text{La}_2\text{Pt}_3\text{Ge}_5$  and (b)  $\text{Pr}_2\text{Pt}_3\text{Ge}_5$ , for which  $M/H$  in terms of  $4\pi\chi$  was measured in an applied field of  $H = 1$  mT parallel to the  $c$ -axis. FC and ZFC stand for field-cooled and zero-field-cooled measurements, respectively. The superconductivity volume fractions in both compounds are less than 2% at 2 K.



**Fig. 4.** (a) and (b) Magnetization susceptibility of  $\text{Pr}_2\text{Pt}_3\text{Ge}_5$  and  $\text{Ce}_2\text{Pt}_3\text{Ge}_5$  single crystals measured in applied magnetic fields along the  $ab$ -plane and  $c$ -axis in the low temperature region ( $2 \text{ K} \leq T \leq 10 \text{ K}$ ), respectively. (c) Inverse magnetic susceptibility of  $\text{Ce}_2\text{Pt}_3\text{Ge}_5$  and  $\text{Pr}_2\text{Pt}_3\text{Ge}_5$  in a temperature range of  $2 \text{ K} \leq T \leq 300 \text{ K}$ . Curie-Weiss fits were performed at temperatures above 150 K. (d) and (e) Field dependence of isothermal magnetization at  $T = 2$  K and 5 K with an applied field along the  $c$ -axis for  $\text{Ce}_2\text{Pt}_3\text{Ge}_5$  and  $\text{Pr}_2\text{Pt}_3\text{Ge}_5$  single crystals, respectively.

As displayed in Fig. 4(b),  $\text{Ce}_2\text{Pt}_3\text{Ge}_5$  shows a clear AFM transition at  $T_N = 3.8$  K. In the normal state, the magnetization in the  $ab$ -plane is stronger than that along the  $c$ -axis. The magnetic moment orientation in the ordered state is thus likely to be lying in the  $ab$ -plane, which is different from its related compound  $\text{Ce}_2\text{Pd}_3\text{Ge}_5$  that is oriented along the  $bc$ -plane, corresponding to the easy direction produced by the CEF.<sup>[23]</sup>

Magnetization along the  $c$ -axis for both  $\text{Pr}_2\text{Pt}_3\text{Ge}_5$  and  $\text{Ce}_2\text{Pt}_3\text{Ge}_5$  follows the Curie-Weiss law above 150 K (Fig. 4(c)), consistent with the results in Ref. [6]. Fitting to the Curie-Weiss law,  $M/H = C_0/(T - \theta_{\text{CW}})$ , gives the Curie-Weiss temperature  $\theta_{\text{CW}} = -33.5$  K for  $\text{Pr}_2\text{Pt}_3\text{Ge}_5$ . The

derived Curie constant  $C_0 = \mu_{\text{eff}}^2 N_A / 3k_B$  gives an effective magnetic moment  $\mu_{\text{eff}} = 3.42 \mu_B/\text{Pr}$ , smaller than the Hund rule value of  $3.58 \mu_B$  of  $\text{Pr}^{3+}$  ion. Similarly, we derive  $\theta_{\text{CW}} = -9.27$  K and  $\mu_{\text{eff}} = 2.59 \mu_B/\text{Ce}$  for  $\text{Ce}_2\text{Pt}_3\text{Ge}_5$ , close to Hund's rule value of  $2.54 \mu_B$  of  $\text{Ce}^{3+}$  ion. An anomaly around 20 K in magnetization for  $\text{Pr}_2\text{Pt}_3\text{Ge}_5$  in the field of  $H = 0.1$  T is observed. The isothermal magnetization measurements of  $\text{Pr}_2\text{Pt}_3\text{Ge}_5$  with the applied magnetic fields along the  $c$ -axis are displayed in Fig. 4(e). At 2 K, well within the AFM state, increasing the field results in a non-linear increase in the magnetization up to 2.4 T where the magnetization clearly changes to a paramagnetic linear behavior. At 5 K,  $\text{Ce}_2\text{Pt}_3\text{Ge}_5$  ex-

hibits a paramagnetic linear field dependence for all applied fields.  $\text{Ce}_2\text{Pt}_3\text{Ge}_5$  also exhibits a similar behavior, as shown in Fig. 4(d) with the critical field at 2 T.

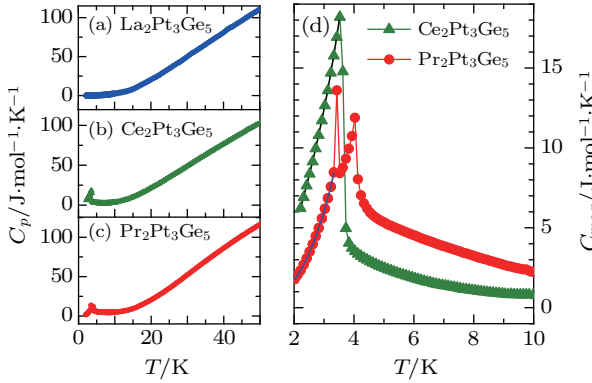


**Fig. 5.** (a)–(c) Temperature dependence of specific heat  $C_p$  of  $\text{La}_2\text{Pt}_3\text{Ge}_5$ ,  $\text{Ce}_2\text{Pt}_3\text{Ge}_5$ , and  $\text{Pr}_2\text{Pt}_3\text{Ge}_5$ , respectively. (d) Magnetic contribution of specific heat of single crystals  $\text{Pr}_2\text{Pt}_3\text{Ge}_5$  and  $\text{Ce}_2\text{Pt}_3\text{Ge}_5$ .

Figures 5(a)–5(c) display the specific heat data  $C_p$  for  $\text{La}_2\text{Pt}_3\text{Ge}_5$ ,  $\text{Pr}_2\text{Pt}_3\text{Ge}_5$ , and  $\text{Ce}_2\text{Pt}_3\text{Ge}_5$ . The normal state temperature dependence of the heat capacity is well described by the expression  $C_p = \gamma_n T + \beta_n T^3$ , with the first and the second terms corresponding to the electronic and phononic contributions, respectively. The derived values of  $\gamma_n$  suggest that both  $\text{Pr}_2\text{Pt}_3\text{Ge}_5$  and  $\text{Ce}_2\text{Pt}_3\text{Ge}_5$  are not heavy fermion compounds. The Debye temperature is derived by the relation<sup>[24]</sup>

$$\theta_D = \left( \frac{12\pi^4 N_A n k_B}{5\beta_n} \right)^{1/3}, \quad (1)$$

where  $N_A$  is the Avogadro constant,  $n$  stands for the number of atoms per formula unit, and  $k_B$  is the Boltzmann constant. All of the derived parameters are summarized in Table 2.

**Table 2.** Parameters derived from specific heat measurements of  $R_2\text{Pt}_3\text{Ge}_5$  ( $R = \text{La}, \text{Ce}, \text{Pr}$ ) in their normal state. Fit range: 10–25 K for  $\text{La}_2\text{Pt}_3\text{Ge}_5$ , 15–20 K for  $\text{Ce}_2\text{Pt}_3\text{Ge}_5$ , and 10–20 K for  $\text{Pr}_2\text{Pt}_3\text{Ge}_5$ .

	$\gamma_n$ / $\text{mJ}\cdot\text{mol}^{-1}\cdot\text{K}^{-2}$	$\beta_n$ / $\text{mJ}\cdot\text{mol}^{-1}\cdot\text{K}^{-4}$	$\theta_D/\text{K}$
$\text{La}_2\text{Pt}_3\text{Ge}_5$	6.6	2.45	199.4
$\text{Ce}_2\text{Pt}_3\text{Ge}_5$	159	2.33	202.8
$\text{Pr}_2\text{Pt}_3\text{Ge}_5$	129	2.26	204.8

The magnetic contribution to specific heat  $C_{\text{mag}}$  of  $\text{Pr}_2\text{Pt}_3\text{Ge}_5$  and  $\text{Ce}_2\text{Pt}_3\text{Ge}_5$  is obtained by subtracting  $C_p$  of  $\text{La}_2\text{Pt}_3\text{Ge}_5$ , the same treatment that has been applied for  $\text{Pr}_2\text{Pd}_3\text{Ge}_5$ .<sup>[25]</sup> As shown in Fig. 5(a), there are clear jumps in the specific heat at temperatures corresponding to the AFM transitions in  $\text{Pr}_2\text{Pt}_3\text{Ge}_5$  and  $\text{Ce}_2\text{Pt}_3\text{Ge}_5$ . The low-temperature regime of  $C_{\text{mag}}$  in the AFM ordered state of  $\text{Pr}_2\text{Pt}_3\text{Ge}_5$  (2–3.2 K) can be well described by  $C_{\text{mag}} = \gamma_m T + \beta_m T^3 \exp(-E_m/k_B T)$ . The fit gives  $\gamma_m = 154 \text{ mJ}\cdot\text{mol}^{-1}\cdot\text{K}^{-2}$  and  $\beta_m = 22 \text{ mJ}\cdot\text{mol}^{-1}\cdot\text{K}^{-4}$ . The latter term represents the contribution of AFM magnons. The positive value of  $E_m = 0.08 \text{ meV}$  for  $\text{Pr}_2\text{Pt}_3\text{Ge}_5$  represents a gap in the magnon

spectrum in the AFM state. The opening of such a gap in the magnon spectrum could lead to anisotropic magnetic behaviors.<sup>[25]</sup> The presence of such anisotropy is confirmed in our magnetic susceptibility measurements (Fig. 4). A similar behavior is also observed in  $\text{Pr}_2\text{Pd}_3\text{Ge}_5$ , indicating that they share similar AFM energy structures. The energy gap of  $\text{Pr}_2\text{Pt}_3\text{Ge}_5$ , however, is smaller than that of  $\text{Pr}_2\text{Pd}_3\text{Ge}_5$ .<sup>[25]</sup> Such a gap is not present in  $\text{Ce}_2\text{Pt}_3\text{Ge}_5$  as the fit does not work well.

One of the most widely accepted methods to determine bulk superconductivity is a jump in the specific heat. While previous literature shows this jump for  $\text{La}_2\text{Pt}_3\text{Ge}_5$ , there is no suitable data for  $\text{Pr}_2\text{Pt}_3\text{Ge}_5$ .<sup>[6]</sup> Therefore, we attempted to isolate the magnetic contribution of specific heat for  $\text{Pr}_2\text{Pt}_3\text{Ge}_5$  by subtracting the phonon contribution  $\beta_n T^3$ . However, this analysis results in no peak, and is not as suitable as the specific heat shows a broad upward curvature due to the AFM. Therefore, we also used  $\text{La}_2\text{Pt}_3\text{Ge}_5$  as a non-magnetic reference compound and subtracted its specific heat from  $\text{Pr}_2\text{Pt}_3\text{Ge}_5$ . Even in this case, there is no peak observed near  $T_c$ . From the detailed analysis of the specific heat, our results suggest that  $\text{Pr}_2\text{Pt}_3\text{Ge}_5$  might have filamentary or impurity-phase-induced superconductivity, similar to some compounds with strain-stabilized non bulk-superconductivity, such as Sn-flux synthesized single crystalline  $\text{YFe}_2\text{Ge}_2$ .<sup>[26]</sup>

It is worth mentioning that the synthesis methods can affect whether bulk or non-bulk superconductivity is in certain compounds. For example, the stoichiometric iron pnictide  $\text{CaFe}_2\text{As}_2$  synthesized by the furnace-cooled method does not show any diamagnetic signal while the quenched sample shows pronounced bulk superconductivity.<sup>[27]</sup> It is thus possible that  $R_2\text{Pt}_3\text{Ge}_5$  ( $R = \text{La}, \text{Ce}, \text{Pr}$ ) might show bulk superconductivity with other different synthesis methods. However, it is beyond the scope of this manuscript to find new methods of making single crystalline  $R_2\text{Pt}_3\text{Ge}_5$  ( $R = \text{La}, \text{Ce}, \text{Pr}$ ).

Another possible origin of the observed superconductivity in  $\text{La}_2\text{Pt}_3\text{Ge}_5$  and  $\text{Pr}_2\text{Pt}_3\text{Ge}_5$  might be the superconducting 1–4–12 filled-skutterudite impurity phases. The self-flux sample synthesis reported used the atomic ratio of 1:4:20, which is the same ratio used to synthesize the filled skutterudite family of materials.<sup>[16]</sup>  $\text{LaPt}_4\text{Ge}_{12}$  and  $\text{PrPt}_4\text{Ge}_{12}$  both show bulk superconductivity around 8 K,<sup>[15]</sup> which is the same as the reported  $T_c$ 's in  $\text{La}_2\text{Pt}_3\text{Ge}_5$  and  $\text{Pr}_2\text{Pt}_3\text{Ge}_5$ . However, the previous work reported a tiny heat capacity jump without entropy conservation below  $T_c$  in  $\text{La}_2\text{Pt}_3\text{Ge}_5$ .<sup>[6]</sup> Moreover,  $\text{La}_2\text{Pt}_3\text{Ge}_5/\text{Pr}_2\text{Pt}_3\text{Ge}_5$  probably have similar upper critical field  $\mu_0 H_{c2}$  values as those of  $\text{LaPt}_4\text{Ge}_{12}/\text{PrPt}_4\text{Ge}_{12}$ . The  $\mu_0 H_{c2}$  is 1.60 T for  $\text{LaPt}_4\text{Ge}_{12}$  and 2.06 T for  $\text{PrPt}_4\text{Ge}_{12}$ .<sup>[15]</sup> Although there is no  $H_{c2}$  data reported for  $\text{La}_2\text{Pt}_3\text{Ge}_5$ , superconductivity can be suppressed by an applied field of 2 T.<sup>[6]</sup> Also, the extrapolated  $H_{c2}$  of  $\text{Pr}_2\text{Pt}_3\text{Ge}_5$  at 0 K is close to that of  $\text{PrPt}_4\text{Ge}_{12}$ .<sup>[10]</sup> We therefore suggest that the origin of the



observed superconductivity in  $\text{Pr}_2\text{Pt}_3\text{Ge}_5$  is not intrinsic according to the heat capacity measurements.

#### 4. Conclusion

In summary, single crystalline ternary germanide compounds  $R_2\text{Pt}_3\text{Ge}_5$  ( $R = \text{La}, \text{Ce}, \text{Pr}$ ) were synthesized using the self-flux method. For  $\text{Pr}_2\text{Pt}_3\text{Ge}_5$ , non-bulk superconductivity is suggested based upon the low superconductivity volume fractions and the absence of obvious superconducting specific heat jumps around  $T_c$  as determined from the resistivity measurements. Antiferromagnetic (AFM) transitions are observed at  $T_{N1} = 4.2$  K and  $T_{N2} = 3.5$  K in  $\text{Pr}_2\text{Pt}_3\text{Ge}_5$ , while  $\text{Ce}_2\text{Pt}_3\text{Ge}_5$  possess only one AFM transition at  $T_N = 3.8$  K.

#### References

- [1] Hossain Z, Ohmoto H, Umeo K, Iga F, Suzuki T, Takabatake T, Takamoto N and Kindo K 1999 *Phys. Rev. B* **60** 10383
- [2] Singh Y, Ramakrishnan S, Hossain Z and Geibel C 2002 *Phys. Rev. B* **66** 014415
- [3] Ramakrishnan S, Patil N G, Aravind D C and Marathe V R 2001 *Phys. Rev. B* **64** 064514
- [4] Schilling A, Cantoni M, Guo J and Ott H R 1993 *Nature* **363** 56
- [5] Wang W, Liu Y, Yang J, Du H, Ning W, Ling L, Tong W, Qu Z, Yang Z, Tian M and Zhang Y 2016 *Chin. Phys. Lett.* **33** 057401
- [6] Sung N H, Roh C J, Kim K S and Cho B K 2012 *Phys. Rev. B* **86** 224507
- [7] Vining C B, Shelton R N, Braun H F and Pelizzon M 1983 *Phys. Rev. B* **27** 2800
- [8] Nakashima M, Kohara H, Thamizhavel A, Matsuda T D, Haga Y, Hedo M, Uwatoko Y, Settai R and Onuki Y 2005 *J. Phys.:Condens. Matter* **17** 4539
- [9] Chen Y, Weng Z, Michael S, Lu X and Yuan H. 2016 *Chin. Phys. B* **25** 077401
- [10] Mazzone D G, Sibille R, Gavilano J L, Bartkowiak M, Mansson M, Frontzek M, Zaharko O, Schefer J and Kenzelmann M 2015 arXiv:1508.02649
- [11] White B D, Thompson J D and Maple M B 2015 *Physica C* **514** 246
- [12] Schlabit W, Baumann J, Pollit B, Rauchschalbe U, Mayer H M, Ahlheim U and Bredl C D 1986 *Physik B* **62** 171
- [13] Maple M B, Frederick N A, Ho P C, Yuhasz W M and Yanagisawa T 2002 *Phys. Rev. B* **65** 100506
- [14] Maple M B, Henkie Z, Yuhasz W M, Ho P C, Yanagisawa T, Sayles T A, Butch N P, Jeffries J R and Pietraszko A 2003 *Physica B* **310** 182
- [15] Gumeniuk R, Schnelle W, Rosner H, Nicklas M, Leithejasper A and Grin Y 2008 *Phys. Rev. Lett.* **100** 017002
- [16] Gumeniuk R, Borrmann H, Ormeci A, Rosner H, Schnelle W, Nicklas M, Grin Y and Leithe-Jasper A 2010 *Z. Kristallogr.* **225** 531
- [17] Zhang J L, Chen Y, Jiao L, Gumeniuk R, Nicklas M, Chen Y H, Yang L, Fu B H, Schnelle W, Rosner H, Leithe-Jasper A, Grin Y, Steglich F and Yuan H Q 2013 *Phys. Rev. B* **87** 064502
- [18] Gumeniuk R, Kvashnina K O, Schnelle W, Nicklas M, Borrmann H, Rosner H, Skourski Y, Tsirlin A A, Leithe-Jasper A and Grin Y 2011 *J. Phys.: Condens. Matter* **23** 465601
- [19] Venkateswarlu D, Samatham S S, Gangrade Mohan and Ganesan V 2014 *J. Phys.: Conf. Ser.* **534** 012040
- [20] Larson A C and Von Dreele R B *GSAS*
- [21] Toby B H 2002 *J. Appl. Crystallogr.* **34** 210
- [22] Becker B, Ramakrishnan S, Groten D, Sllow S, Mattheus C C, Nieuwenhuys G J and Mydosh J A 1997 *Physica B* **230** 253
- [23] Feyerherm R, Becker B, Collins M F, Mydosh J, Nieuwenhuys G J and Ramakrishnan S 1997 *Physica B* **241** 643
- [24] Sangeetha N S, Thamizhavel A, Tomy C V, Basu S, Ramakrishnan S and Pal D 2011 *Phys. Rev. B* **84** 064430
- [25] Anand V K, Hossain Z and Geibel C 2008 *Phys. Rev. B* **77** 184407
- [26] Kim S H, Ran S, Mun E D, Hodovanets H, Tanatar M A, Prozorov R, Budako S L and Canfield P C 2015 *Philos. Mag.* **95** 804
- [27] Chen D Y, Yu J, Ruan B B, Guo Q, Zhang L, Mu Q G, Wang X C, Pan B J, Chen G F and Ren Z A 2016 *Chin. Phys. Lett.* **33** 67402